Photonic Band Gap and Light Routing in Self-Assembled Lattices of Epitaxial Ge-on-Si Microstructures

Jacopo Pedrini,[1,*] Andrea Barzaghi,[2] Joao Valente,[3] Douglas J. Paul,[3] Giovanni Isella,[2] and Fabio Pezzoli[1]

[1] *L-NESS and Università degli Studi di Milano-Bicocca, Dipartimento di Scienza dei Materiali, via Cozzi, 55, Milano 20125, Italy*

[2] *L-NESS and Politecnico di Milano, Via Anzani, 42, Como 22100, Italy*

[3] *University of Glasgow, James Watt School of Engineering, Rankine Building, Oakfield Avenue, Glasgow G12 8LT, United Kingdom*

(Received 16 July 2021; revised 28 October 2021; accepted 18 November 2021; published 9 December 2021)

The emergence of a photonic band gap in Ge-on-Si micropillars ordered in a two-dimensional square lattice is demonstrated by the finite-element method. Candidate architectures are fabricated through epitaxy and the opening of the photonic band gap experimentally proved by photoluminescence spectroscopy. When the direct-gap emission of Ge is resonantly driven into the photonic gap, light propagation in the lattice plane is inhibited. Emission is eventually funneled out of plane, yielding a giant increase, i.e., about one order of magnitude, in the observed intensity. The demonstration of light routing in microcrystals' lattices opens interesting possibilities for Si photonics. The epitaxial self-assembled microstructures introduced here can be monotonically integrated on Si to improve the performances of group-IV lasers or engineered to optimize the working wavelength of future quantum photonic circuits.

DOI: 10.1103/PhysRevApplied.16.064024

I. INTRODUCTION

Photonic crystals (PCs) are amongst the most useful components for light management. They allow routing and storage of the photon flux when utilized as waveguides or cavities in passive photonic circuits [1], but they can also be applied to active components, e.g., lasers, as performance boosters [2]. The most common and easiest way to realize PCs consists of creating voids in the form of two-dimensional (2D) lattices in a thin semiconductor slab. In such structures, the photonic properties are determined by the in-plane modulation of the refractive index, while the abrupt out-of-plane discontinuity confines light transport within the semiconductor membrane. Such 2D PCs are commonly fabricated via electron-beam lithography followed by chemical etching. This process is extremely precise, resulting in almost perfect geometries, but fine control of the etching step can be difficult to achieve, introducing roughness and potential sources of scattering and optical losses. All these side effects are detrimental in the quest for large-scale photonics. A possible solution to these issues is to exploit a bottom-up approach that imprints the photonic layout through direct epitaxial growth of high-quality structures. Hence, epitaxy represents a promising but overlooked approach for the development of high-quality PCs. Epitaxy yields atomically smooth surfaces that are unmatched in terms of roughness and concentration of nonradiative centers. Unfortunately, conventional deposition techniques often rely on random growth, which hinders their applicability to the manufacture of periodically ordered structures. Presently, the exploitation of functional epitaxy to realize 2D PCs has not been convincingly demonstrated, and motivates a drastic change in perspective.

Here we turn our attention to the out-of-equilibrium deposition on pillar-patterned templates. This approach allows the direct growth on Si of high-quality semiconductor monocrystals at the micrometer scale [3–9]. Such micron-sized grains are all equally oriented and self-ordered thanks to the periodic nature of the patterned seeds that allow mutual shadowing and eventually limit the lateral expansion. This promotes crystal elongation along the normal to the substrate surface [10], achieving well-controlled and very-narrow, i.e., down to few tens of nm, separations between neighboring grains. Such self-assembled microcrystals present several interesting properties that make them particularly attractive for the epitaxial implementation of group-IV photonics. The periodic nature of the pattern transferred onto the Si substrate and the high refractive index of group-IV semiconductors composing the microcrystals are two key-enabling

*jacopo.pedrini@unimib.it

properties for realizing PCs. Furthermore, the fabrication technique is particularly appealing for the photonic industry because it can combine wide-field lithography to prepare the templates and rapid, out-of-equilibrium epitaxy to realize photonic components, unleashing faster and higher throughput than conventional PC fabrication strategies [3,10].

The detailed investigation of the emergence of photonic effects in epitaxial self-assembled microcrystals is, however, at an early stage [9]. To demonstrate our proposed concept, we compute the photonic band structure of an experimentally feasible 2D PC consisting of a square matrix of Ge microcrystals on top of periodic Si pillars (see the scheme in Fig. 1). A finite-element-method (FEM) simulation of the cross-section high-symmetry planes passing through the microcrystal centers shows the presence of a full photonic band gap (PBG) centered at 0.870 eV. The PBG prohibits in-plane propagation and can be exploited to reroute light towards the top surface of the heterostructure, achieving directional vertical emission. We experimentally verify this effect by leveraging the direct-gap PL of Ge in a backscattering configuration as a sensitive probe. We also utilize temperature as a suitable turning knob to control the frequency detuning, Δ, with the expected PBG. At resonance, the enhancement observed in the PL intensity with respect to the experiment conducted on an unpatterned Ge film is about one order of magnitude. This provides striking evidences of the band-gap opening and of the consequent photonic mediated directional emission enabled by the microcrystal configuration. This principle, combined with the flexibility of our fabrication technique can be extended to various materials, opening fields of application for epitaxial microcrystals in Si photonics with possible implications in diverse fields such as quantum information [11], sensing [12], signal processing [13], spectroscopy [14], and imaging [15].

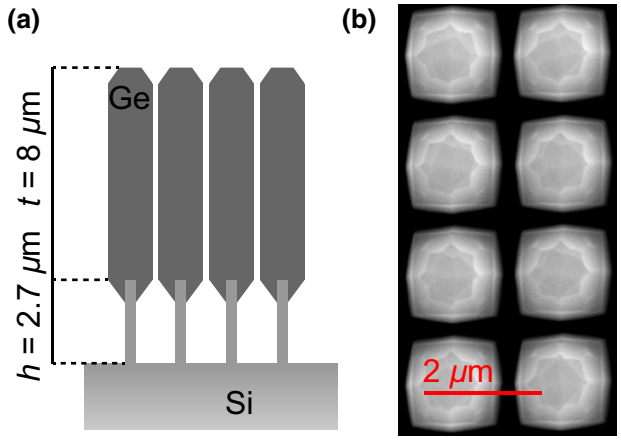

FIG. 1. (a) Scheme of the microcrystals' geometry. 8-μm-thick Ge microcrystals are epitaxially grown on 2.7-μm-thick Si pillar seeds with lateral size 0.25 μm and interpillar distance 1.5 μm (not to scale). (b) Top-down SEM image showing a rectangular portion of the sample area containing the microcrystal matrix.

II. METHODS

A. Numerical modeling

The numerical analysis is carried out using COMSOL Multiphysics, a commercial software implementing the FEM. Cross-section 2D simulations are performed because of the in-plane symmetry of the microcrystal matrix. The eigenfrequency of the photonic modes is calculated by sweeping the wave vector k through high-symmetry points of the square Brillouin zone for the out-of-plane polarization of the electric field (TM modes). The optical constants of Ge are considered to be wavelength independent and equal to the value they assume at 0.870 eV. The values of the optical constants are extracted from the literature [16] and are $n = 4.22$, $k = 1.8 \times 10^{-4}$ for Ge and $n = 1$, $k = 0$ for the vacuum surrounding the microcrystal. The electronic band structure of Ge is modeled with a commercial $k \cdot p$ software. We use different directions in k space, i.e., from [000] to [001], [111] and [011] for both strained and relaxed material.

B. Sample preparation

Ge microcrystals are grown on patterned substrates by low-energy plasma-enhanced chemical vapor deposition [17]. Figure 1(a) shows a schematic of the microcrystal structure. Square silicon chips (15×15 cm^2) are patterned via electron beam lithography. Pillars with 250-nm lateral size with 1.5-μm spacing are patterned using a 700-nm high-purity silsesquioxane (HSQ) layer. Beam current is kept at 4 nA and the dose is 1600 μC cm^{-2}. After development in tetramethylammonium hydroxide (TMAH) and plasma ash, substrates are reactive ion etched for 8 min using C_4F_8 and SF_6 gases at 600 W. Such a process presents a selectivity to the electron-beam resist of 10:1 and achieves a final pillar height of 2.7 μm. Such processes are very reproducible and provide mechanically stable pillars down to 250 nm, even for larger gaps.

The square pillars, with lateral size of 250 nm, are separated by a 1.5-μm gap. The overall patterned area of the sample is approximately 100×100 μm^2, which is larger than the spot size of the laser used for the PL measurements. The Ge deposition is performed at 450 °C with a growth rate of 5 nm/s for a total thickness of 8 μm. During growth, Ge microcrystals nucleate on each etched Si seed. At first, the microcrystals expand both laterally and vertically. As the deposition proceeds, vertical growth is established, leading to the development of Ge microcrystals separated by air gaps of approximately 200 nm, as shown in the top-down SEM micrograph reported in

Fig. 1(b). Notably, the simultaneous growth on unprocessed areas of the same wafer provides us with the reference, namely an unpatterned Ge-on-Si film, which enables us to discriminate between material-induced features and pattern-induced effects.

C. Optical characterization

PL measurements are performed at variable temperatures from 5 to 300 K. Samples are mounted in a closed-cycle cryostat and excited with a 1064-nm $Nd:YVO_4$ continuous-wave laser. The excitation power is focussed on a spot with a 50-μm diameter, resulting in an excitation power density of approximately 4 kW cm^{-2}, which guarantees negligible light-induced heating of the microcrystals. The PL is collected in a backscattering geometry with a single-grating spectrograph equipped with a liquid-N_2 cooled (In, Ga)As array. The spectral pitch is less than 1 meV/pixel.

III. RESULTS AND DISCUSSION

A. Design and modeling

We performed 2D FEM calculations using a unit cell containing a microcrystal structure with periodic boundary conditions to simulate the photonic properties of a realistic Ge-on-Si heterostructure. The scheme of the unit cell is shown in the inset of Fig. 2(a). The periodic repetition in a 2D lattice of such a unit cell mimics the microcrystal matrix that is reported in the scanning electron microscopy image of Fig. 1(b). The lattice has a square

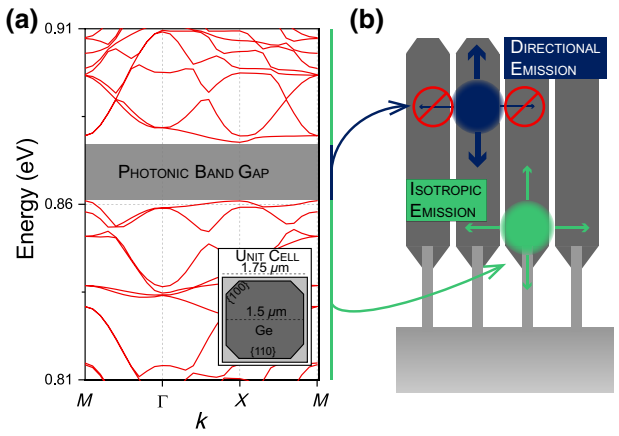

FIG. 2. (a) Simulated photonic band structure of the microcrystal array for the TM polarization. A full photonic band gap centered at about 0.870 eV is highlighted. Inset: scheme of the simulated 2D structure. (b) Cross-section sketch of the microcrystal array (not to scale) highlighting the process of the forbidden propagation and directional emission of light propagating at frequencies inside the bandwidth of the photonic band gap (blue) and of isotropic emission of light at frequencies outside the gap (green).

Brillouin zone where X, Γ, and M are the high-symmetry points [18]. Due to the in-plane symmetry, we simulate a cross section of the Ge microcrystal parallel to the top (001) surface. The Ge microcrystal is bounded by {110} and {100} facets, resulting in the pseudo-octagonal shape reported in the inset of Fig. 2(a). The size of the {110} and {100} facets is 1.3 μm and 140 nm, respectively. The actual microcrystal morphology can be slightly more complicated presenting rounder edges due to the development of higher-index facets, but because of their minor extension these facets introduce only minor corrections and can be neglected, as reported in Fig. S1 (see Supplemental Material [19]) that shows the band-structure calculation for different microcrystal cross sections.

As shown in Fig. 2(a), the band structure presents a large number of high-frequency modes due to the large size of the microcrystals. Interestingly, a full PBG opens up at 0.870 eV with a width of approximately 17 meV. The PBG is the key parameter for the applicability of the PC to optical devices, because it allows light control and management. In the particular case of the microcrystal matrix, such a PBG is expected to generate a stop band for light transport along the in-plane directions. Photons with energy outside the PBG will then propagate isotropically, whereas radiative decay events at frequencies matching the PBG will be inhibited while being redistributed towards the out-of-plane directions [20]. This will manifest itself in an enhancement of the rate of light emitted outside the 2D plane, yielding directional propagation along the microcrystal growth axis. A schematic representation of isotropic and directional propagation at two wavelengths, outside and inside the PBG, is shown in Fig. 2(b). This principle could be exploited to reduce optical losses and to enhance the extraction efficiency in high-refractive-index materials such as group-IV semiconductors. It is worth noting that the PBG is present only for the TM polarization, i.e., for emitted light that has an out-of-plane component of the electric field. Indeed, Fig. S1 within the Supplemental Material [19] shows that the photonic band structure for the TE-polarized light does not have a PBG in the range of interest and thus can propagate along the sample surface. In our structure a PBG is thus present only for the TM polarization, so that the resulting TM stop band will be the only contribution to the enhancement of the light extraction efficiency discussed hereafter.

B. Experimental proof

Self-assembled, epitaxial microcrystals have already shown interesting optical properties [6,7,9]. Here we experimentally explore the interaction of their light emission with the PC structure predicted by FEM. We thus focus on the direct band-gap recombination in Ge, being motivated by its strong potential from the standpoint of

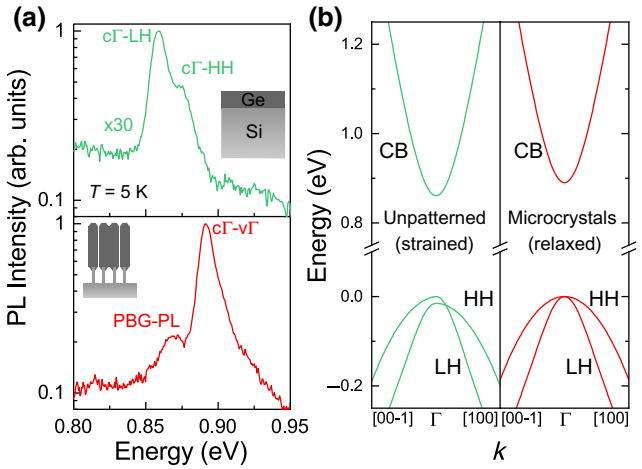

FIG. 3. (a) Continuous-wave photoluminescence spectra measured at 5 K in an 8-μm-thick unpatterned Ge epilayer on Si (top, green line) and 8-μm-thick Ge microcrystals (bottom, red line) under 1064-nm excitation. The spectrum of the unpatterned Ge epilayer is magnified 30×. (b) Left: calculated electronic band structure of the unpatterned Ge epilayer under thermal tensile strain (green lines). It can be seen the lifting of the degeneracy between heavy-hole (HH) and light-hole (LH) bands at the top of the valence band. Right: simulated electronic band structure of a fully relaxed Ge microcrystal (red lines) highlighting the bulklike valence-band degeneracy at the zone center.

group-IV photonic components [21,22]. To verify the presence of the PBG we perform continuous-wave PL experiments on the microcrystals, comparing the results with those obtained on the reference unpatterned layer [23]. The comparison is useful to discriminate the effect of the material from that of the microstructure. To ensure that the microcrystals and the reference Ge film have the same material properties, we measure the PL of the epilayer in an unpatterned region of the same chip on which the fabrication process is performed. The PL spectra measured at 5 K are reported in Fig. 3(a) and present noticeable differences. The PL intensity of the microcrystals turns out to be approximately 30 times higher than that of the unpatterned film. This difference is observed with good reproducibility on other samples and mostly results from the superior optical quality of the microcrystals, which is determined by the mitigation of nonradiative recombination centers due to blocking and expulsion at the sidewalls of the threading dislocations [6].

Another major difference between the two samples can be found in the energy position of the direct-band-gap recombination. The unpatterned Ge epilayer shows a main structure at 0.858 eV and a weaker shoulder at 0.873 eV, while the microcrystals' PL is dominated by a bright recombination at 0.891 eV, accompanied by a lower intensity feature at 0.870 eV. To understand the presence of the two distinct contributions in the unpatterned Ge we take into account the tensile strain resulting from the thermal mismatch with the Si substrate [24]. This has a strong effect on the band structure of Ge since it induces a redshift and it breaks the valence-band degeneracy at the center of the Brillouin zone [23], as shown in the calculated band structure reported in Fig. 3(b). The two PL structures observed in the top panel of Fig. 3(a) can thus be ascribed to radiative pathways at the center Γ of the Brillouin zone from the bottom of the conduction band (cΓ) towards heavy-hole (HH) and light-hole (LH) bands, respectively. The 0.873-eV peak arises from the cΓ-HH transition, while the 0.858-eV structure stems from the cΓ-LH recombination [23]. As opposed to the case of the unpatterned Ge, the calculated electronic band structure [see Fig. 3(b)] of the epitaxial microcrystals does not feature HH-LH splitting, because the tensile strain is fully relaxed through the three-dimensional growth of the microcrystals [3]. The direct recombination of the strain-free Ge microcrystals thus occurs at higher energy than in the unpatterned epilayer and can be associated to the prominent peak at 0.891 eV. The presence of a lower-energy structure in the microcrystal PL is instead unexpected, because its energy by far exceeds the one of the indirect gap (approximately 0.74 eV [25]). In addition, a direct comparison with the PL of bulk materials rules out electronic Raman scattering as another potential source of its origin [26] (see Fig. S2 within the Supplemental Material [19]). It is worth noting, however, that the energy and the linewidth (FWHM approximately 20 meV) of this spectral feature agree strikingly well with those of the PBG obtained from the FEM simulations. The analysis of the PL lineshape and position as a function of temperature allows us to further understand the origin of the PL components observed at 5 K.

At first, we focus on the temperature-induced dependence of the emission energy, shown in Figs. 4(a)–4(c). The raw PL spectra of the Ge epilayer and of the microcrystals as a function of temperature are reported in Figs. S3 and S4 within the Supplemental Material [19]. The two PL peaks pertaining to the reference Ge epilayer redshift, demonstrating band-gap narrowing and confirming that these are interband transitions across the Ge direct gap. The deviation of the cΓ-LH line from Varshni's law [25] observed above 100 K and its merging with the cΓ-HH recombination can be rationalized by considering a thermally activated LH-HH repopulation mechanism. This behavior is consistent with previous reports on μm-thick Ge-on-Si epilayers [23,27]. It should be noted that the presence of a single data point between 125 and 200 K is due to the extremely broad and low-intensity PL line that does not allow us to extract with satisfactory confidence the LH and HH recombination energies (see Fig. S5 within the Supplemental Material [19]). The temperature dependence of the PL of Ge microcrystals shows, conversely, a more subtle scenario since the two peaks behave very differently with the increasing temperature. Figures 4(b) and 4(c) show that the feature at 0.891 eV demonstrates

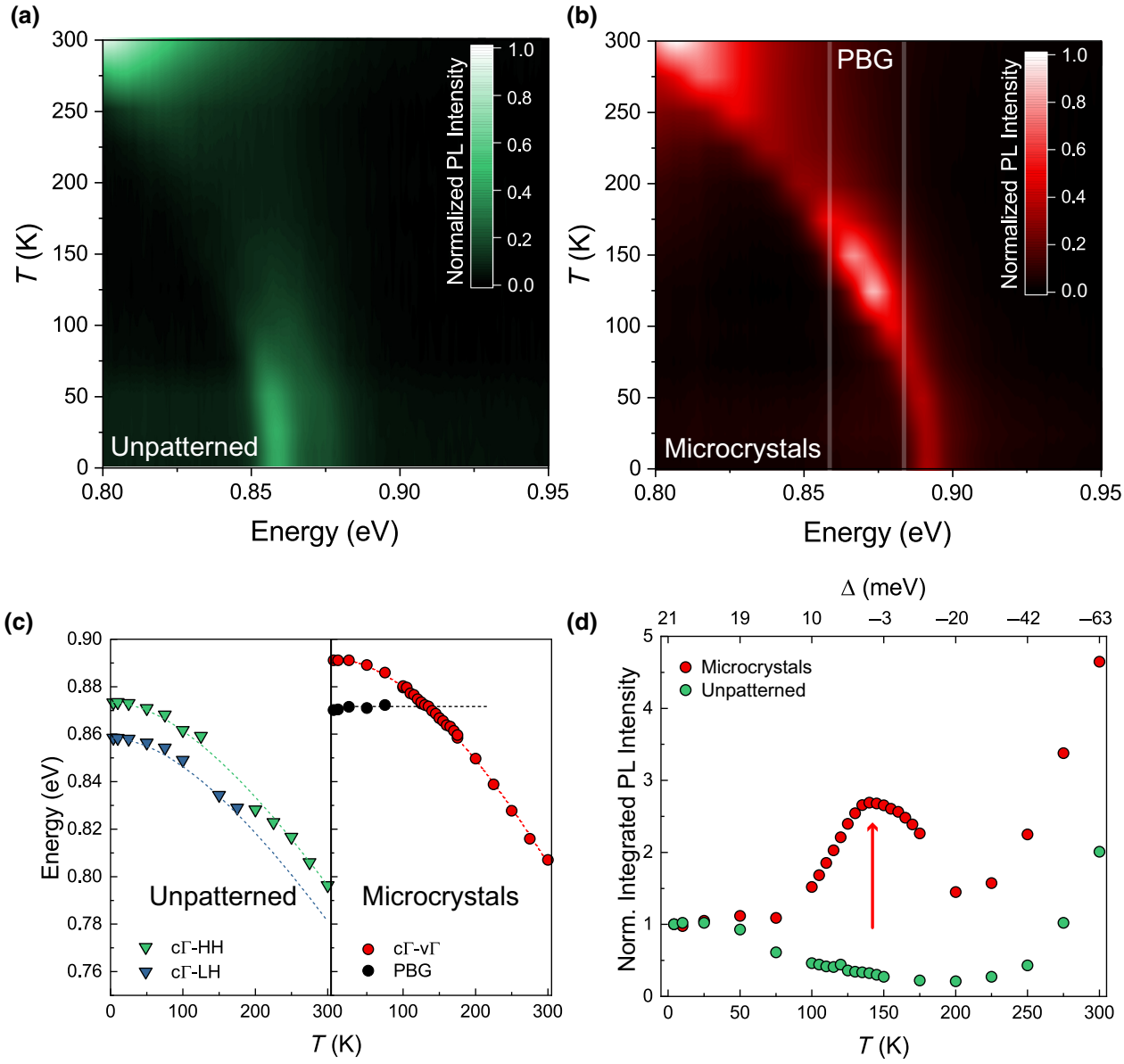

FIG. 4. (a) Color-scale map of the continuous-wave PL of an unpatterned 8-μm-thick Ge epilayer as a function of the lattice temperature under 1064-nm excitation. Temperature ranges from 5 to 300 K. (b) Color-scale map of the continuous-wave PL of 8-μm-thick Ge microcrystals measured under the same experimental conditions of the unpatterned reference. (c) Temperature-dependent redshift of the 8-μm-thick unpatterned Ge epilayer (green and blue) and of the 8-μm-thick Ge microcrystals (red and black). Dashed lines are the Varshni fit of the corresponding experimental PL data. (d) Integrated PL intensity of the direct band-gap recombinations of the 8-μm-thick unpatterned Ge epilayer (green) and of the 8-μm-thick microcrystals (red) normalized for their respective values measured at 5 K. The PL is integrated on the full band of the direct emission over a mobile range, following the redshift of the recombination as a function of temperature.

the expected Varshni's redshift. The energy position of the minor peak remains notably constant at 0.870 eV up to 75 K, being no longer resolved at higher temperatures. The complete absence of any temperature dependence clearly shows that this spectral feature is not an electronic transition. To gather a better understanding of this structure, it is worth having a closer look at the variation of the PL intensity upon the temperature [Fig. 4(d)]. As the temperature increases, the direct-gap PL intensity of a Ge-on-Si epilayer is known to decrease to a minimum at about 200 K and then to gain weight towards room temperature [6,28]. Indeed, at cryogenic temperatures the direct recombination is efficient because both nonradiative recombinations and Γ-L intervalley scattering are negligible. The opposite holds near room temperature, yielding the behavior shown in Fig. 4(d) characterized by an overall intensity minimum

at intermediate temperatures, i.e., about 200 K. In stark contrast, the PL intensity of the microcrystals demonstrates an opposite phenomenon with a well-defined maximum at about 145 K. This puzzling behavior is consistently reproduced on various samples. At 145 K the PL intensity is about 3 times than that at 5 K. Above all it is 8 times larger than the intensity measured at the same temperature in the unpatterned reference, even after having minimized the nonradiative contributions of the dislocations through the PL normalization with respect to the lowest temperature values [see Fig. 4(d)]. It should also be noted that the temperature scan demonstrates that the intensity of the direct-gap PL peak increases sharply right at the onset of the calculated boundaries of the PBG and reaches a maximum at 145 K when the PL peak energy equals 0.870 eV. The drastic PL increase can therefore be interpreted as a redirection of emitted light towards the top of the microcrystals when its energy is brought into resonance with the center of the PBG predicted by FEM simulations. This finally confirms the concept of photonic mediated directional emission as proposed in Fig. 2. The out-of-plane redirection of the light emitted inside of the PBG bandwidth also allows us to ascertain the nature of the low-intensity emission at 0.870 eV observed in the microcrystal PL at low temperatures [see Figs. 3(a) and 4(c)]. Indeed, such a PL structure is most likely given by the low-energy tail of the main direct-gap peak, which falls within the PBG and is guided out of the microcrystals towards the top surface. This contribution, albeit less evident, can be observed also on the high-energy tail of the direct-gap peak in the PL spectra, after the resonance observed at 145 K and up to 250 K, as reported in Figs. S3 and S6 within the Supplemental Material [19].

IV. CONCLUSION

We predict the occurrence of a full PBG in a 2D PC made of semiconductor microcrystals. To experimentally verify its presence, we perform PL measurements of Ge-on-Si heteroepitaxial architectures using temperature as a parameter to control the energy detuning between the PBG and the radiative recombination through the direct gap of Ge. We find about an order of magnitude enhancement of the PL upon resonance, that we interpret as a result of the in-plane stop band generated by the PBG that reroutes the PL towards the direction perpendicular to the periodicity plane, increasing the light extraction efficiency. The demonstration of the presence of a PBG opens an exciting field of application for semiconductor microcrystals self-ordered on patterned substrates. The extremely flexible fabrication technique provides a large number of degrees of freedom in terms of morphology and patterning, that could allow for further improvements of the microstructures. Moreover, by virtue of the inherent transparency of group-IV materials at long wavelengths, we expect that Ge/SiGe quantum-well emitters embedded into microcrystals [29] can have strong potential for the implementation of VCSELs and quantum cascade lasers spanning the mid-infrared and terahertz range [30,31].

ACKNOWLEDGMENTS

We thank Andrea Tamiazzo for the help with the spectroscopic measurements. We thank Francesco Montalenti and Anna Marzegalli for the use of Comsol Multiphysics. This research is funded by the European Commission (Horizon-2020 FET "microSPIRE" project, ID: 766955), and by Regione Lombardia, under the TEINVEIN project, Call Accordi per la Ricerca e l'Innovazione, co-funded by POR FESR 2014-2020 (ID: 242092).

[1] J. D. Joannopoulos, P. R. Villeneuve, and S. Fan, Photonic crystals: Putting a new twist on light, Nature **386**, 143 (1997).

[2] S. Wu, H. Xia, J. Xu, X. Sun, and X. Liu, Manipulating luminescence of light emitters by photonic crystals, Adv. Mater. **30**, 1 (2018).

[3] C. V. Falub, H. Von Känel, F. Isa, R. Bergamaschini, A. Marzegalli, D. Chrastina, G. Isella, E. Müller, P. Niedermann, and L. Miglio, Scaling hetero-epitaxy from layers to three-dimensional crystals, Science **335**, 1330 (2012).

[4] A. Marzegalli, F. Isa, H. Groiss, E. Müller, C. V. Falub, A. G. Taboada, P. Niedermann, G. Isella, F. Schäffler, F. Montalenti, H. Von Känel, and L. Miglio, Unexpected dominance of vertical dislocations in high-misfit Ge/Si(001) films and their elimination by deep substrate patterning, Adv. Mater. **25**, 4408 (2013).

[5] F. Isa, M. Salvalaglio, Y. A. R. Dasilva, M. Meduna, M. Barget, A. Jung, T. Kreiliger, G. Isella, R. Erni, F. Pezzoli, E. Bonera, P. Niedermann, P. Gröning, F. Montalenti, and H. Von Känel, Highly mismatched, dislocation-free SiGe/Si heterostructures, Adv. Mater. **28**, 884 (2016).

[6] F. Pezzoli, F. Isa, G. Isella, C. V. Falub, T. Kreiliger, M. Salvalaglio, R. Bergamaschini, E. Grilli, M. Guzzi, H. Von Känel, and L. Miglio, Ge Crystals on Si Show Their Light, Phys. Rev. Appl. **1**, 1 (2014).

[7] F. Pezzoli, A. Giorgioni, K. Gallacher, F. Isa, P. Biagioni, R. W. Millar, E. Gatti, E. Grilli, E. Bonera, G. Isella, D. J. Paul, and L. Miglio, Disentangling nonradiative recombination processes in Ge micro-crystals on Si substrates, Appl. Phys. Lett. **108**, 262103 (2016).

[8] F. Montalenti, F. Rovaris, R. Bergamaschini, L. Miglio, M. Salvalaglio, G. Isella, F. Isa, and H. V. Känel, Dislocation-free SiGe/Si heterostructures, Crystals **8**, 1 (2018).

[9] J. Pedrini, P. Biagioni, A. Ballabio, A. Barzaghi, M. Bonzi, E. Bonera, G. Isella, and F. Pezzoli, Broadband control of the optical properties of semiconductors through site-controlled self-assembly of microcrystals, Opt. Express **28**, 24981 (2020).

[10] R. Bergamaschini, F. Isa, C. V. Falub, P. Niedermann, E. Müller, G. Isella, H. Von Känel, and L. Miglio, Self-aligned

Ge and SiGe three-dimensional epitaxy on dense Si pillar arrays, Surf. Sci. Rep. **68**, 390 (2013).

[11] J. M. Arrazola, *et al.*, Quantum circuits with many photons on a programmable nanophotonic chip, Nature **591**, 54 (2021).

[12] A. Z. Subramanian, *et al.*, Silicon and silicon nitride photonic circuits for spectroscopic sensing on-a-chip, Photonics Res. **3**, B47 (2015).

[13] H. Zhou, Y. Zhao, X. Wang, D. Gao, J. Dong, and X. Zhang, Self-configuring and reconfigurable silicon photonic signal processor, ACS Photonics **7**, 792 (2020).

[14] B. Bernhardt, A. Ozawa, P. Jacquet, M. Jacquey, Y. Kobayashi, T. Udem, R. Holzwarth, G. Guelachvili, T. W. Hänsch, and N. Picqué, Cavity-enhanced dual-comb spectroscopy, Nat. Photonics **4**, 55 (2010).

[15] C. Rogers, A. Y. Piggott, D. J. Thomson, R. F. Wiser, I. E. Opris, S. A. Fortune, A. J. Compston, A. Gondarenko, F. Meng, X. Chen, G. T. Reed, and R. Nicolaescu, A universal 3D imaging sensor on a silicon photonics platform, Nature **590**, 256 (2020).

[16] T. Amotchkina, M. Trubetskov, D. Hahner, and V. Pervak, Characterization of e-beam evaporated Ge, YbF_3, ZnS, and LaF_3 thin films for laser-oriented coatings, Appl. Opt. **59**, A40 (2020).

[17] C. Rosenblad, H. R. Deller, A. Dommann, T. Meyer, P. Schroeter, and H. von Känel, Silicon epitaxy by low-energy plasma enhanced chemical vapor deposition, J. Vac. Sci. Technol. A Vac. Surf. Film. **16**, 2785 (2002).

[18] J. D. Joannopoulos, *Photonic Crystals: Molding the Flow of Light* (Princeton University Press, Princeton, New Jersey, USA, 2008), 2nd ed.

[19] See Supplemental Material at http://link.aps.org/supplemental/10.1103/PhysRevApplied.16.064024 for additional band-structure calculations and photoluminescence spectra.

[20] M. Fujita, S. Takahashi, Y. Tanaka, T. Asano, and S. Noda, Simultaneous inhibition and redistribution of spontaneous light emission in photonic crystals, Science **308**, 1296 (2005).

[21] F. T. Armand Pilon, A. Lyasota, Y. M. Niquet, V. Reboud, V. Calvo, N. Pauc, J. Widiez, C. Bonzon, J. M. Hartmann, A. Chelnokov, J. Faist, and H. Sigg, Lasing in strained germanium microbridges, Nat. Commun. **10**, 1 (2019).

[22] S. Bao, D. Kim, C. Onwukaeme, S. Gupta, K. Saraswat, K. H. Lee, Y. Kim, D. Min, Y. Jung, H. Qiu, H. Wang, E. A. Fitzgerald, C. S. Tan, and D. Nam, Low-threshold optically pumped lasing in highly strained germanium nanowires, Nat. Commun. **8**, 1 (2017).

[23] E. Vitiello, M. Virgilio, A. Giorgioni, J. Frigerio, E. Gatti, S. De Cesari, E. Bonera, E. Grilli, G. Isella, and F. Pezzoli, Spin-dependent direct gap emission in tensile-strained Ge films on Si substrates, Phys. Rev. B—Condens. Matter Mater. Phys. **92**, 1 (2015).

[24] Y. Ishikawa, K. Wada, J. Liu, D. D. Cannon, H. C. Luan, J. Michel, and L. C. Kimerling, Strain-induced enhancement of near-infrared absorption in Ge epitaxial layers grown on Si substrate, J. Appl. Phys. **98**, 013501 (2005).

[25] Y. P. Varshni, Temperature dependence of the energy gap in semiconductors, Physica **34**, 149 (1967).

[26] F. Pezzoli, A. Balocchi, E. Vitiello, T. Amand, and X. Marie, Optical orientation of electron spins and valence-band spectroscopy in germanium, Phys. Rev. B—Condens. Matter Mater. Phys. **91**, 1 (2015).

[27] J. Liu, L. C. Kimerling, and J. Michel, Monolithic Ge-on-Si lasers for large-scale electronic-photonic integration, Semicond. Sci. Technol. **27**, 094006 (2012).

[28] E. Gatti, E. Grilli, M. Guzzi, D. Chrastina, G. Isella, and H. Von Känel, Room temperature photoluminescence of Ge multiple quantum wells with Ge-rich barriers, Appl. Phys. Lett. **98**, 3 (2011).

[29] F. Isa, F. Pezzoli, G. Isella, M. Meduna, C. V. Falub, E. Müller, T. Kreiliger, A. G. Taboada, H. Von Känel, and L. Miglio, Three-dimensional Ge/SiGe multiple quantum wells deposited on Si(001) and Si(111) patterned substrates, Semicond. Sci. Technol. **30**, 105001 (2015).

[30] C. Ciano, M. Virgilio, L. Bagolini, L. Baldassarre, A. Pashkin, M. Helm, M. Montanari, L. Persichetti, L. Di Gaspare, G. Capellini, D. J. Paul, G. Scalari, J. Faist, M. De Seta, and M. Ortolani, Terahertz absorption-saturation and emission from electron-doped germanium quantum wells, Opt. Express **28**, 7245 (2020).

[31] K. Gallacher, M. Ortolani, K. Rew, C. Ciano, L. Baldassarre, M. Virgilio, G. Scalari, J. Faist, L. Di Gaspare, M. De Seta, G. Capellini, T. Grange, S. Birner, and D. J. Paul, Design and simulation of losses in Ge/SiGe terahertz quantum cascade laser waveguides, Opt. Express **28**, 4786 (2020).